PHYSICAL REVIEW B VOLUME 25, NUMBER 4 15 FEBRUARY 1982

Dynamical correlations in a two-dimensional electron gas: First-order perturbation theory

A. Czachor,* A. Holas,* S. R. Sharma, and K. S. Singwi
Department of Physics and Astronomy, Northwestern University, Evanston, Illinois 60201
(Received 20 July 1981; revised manuscript received 16 October 1981)

First-order Feynman diagrams for the proper polarizability of a two-dimensional electron liquid in the jellium model, valid for arbitrary wave vector and frequency, are evaluated, their singularities and analytical properties are examined, and a reliable numerical procedure for calculating them is established. Quantities such as the dielectric function $\epsilon(\vec{k},\omega)$, the dynamic-complex-local-field factor $G(\vec{k},\omega)$, dynamic structure factor $S(\vec{k},\omega)$, static structure factor $S(\vec{k})$, and the pair correlation function $g(r)$ have been calculated and compared with the corresponding quantities in the random-phase approximation (RPA). Comparison has also been made with the three-dimensional case. A closed expression for the plasmon dispersion within the RPA has been derived. The first-order theory interestingly enough predicts a large enhancement of the static polarizability for $k=2k_F$, which could play an important role in predicting charge-density-wave instabilities in metallic layered compounds.

I. INTRODUCTION

Over the years considerable theoretical effort has gone into the calculation of frequency- and wave-number-dependent dielectric function of a three-dimensional (3D) electron gas in a jellium model. Interest in the analogous problem in a 2D case is of more recent origin. This interest has arisen for two main reasons: (a) it has been possible to realize in the laboratory 2D or quasi-2D electron systems with a continuously variable electron density, and (b) the belief that the 2D systems could exhibit unexpected behavior in some of their properties not forseen from our intuition of the 3D world.

Stern[1] was the first to calculate the lowest-order polarizability $\pi^0(\vec{k},\omega)$ for a 2D electron gas in the random phase approximation (RPA), the 2D analog of the well-known Lindhard function. He found the interesting result that the plasmon dispersion goes to zero as $k^{1/2}$ as the wave number k tends to zero. Since Stern's work some attempts have been made to improve upon his RPA result. Of these the most significant ones are those of Rajagopal[2] and Jonson.[3] The former author evaluated the polarizability, including the exchange processes only, as a power series expansion in $k_F k/m\omega$, k_F being the Fermi wave vector. He was thus able to calculate the correction, arising from exchange only, to the RPA plasmon dispersion. He also calculated the static polarizability $\pi(k,0)$ to order k^2. In a subsequent paper Rajagopal and Kimball[4] calculated the correlation energy in RPA. Jonson extended the self-consistent scheme of Singwi, Tosi, Land, and Sjölander[5] (STLS) to the 2D case and calculated a number of physical quantities including the pair correlation function and compared them with the corresponding quantities in the RPA and Hubbard approximation (HA). His main conclusion was that the RPA and HA are less satisfactory approximations for a 2D than for a 3D case. For a given r_s since the ratio of exchange to kinetic energy is larger in a 2D case compared to that in the 3D case, correlations are more important in the former.

In the calculation of Jonson corrections to the RPA are incorporated through a static local field $G(k)$ in the polarization which is a good approximation so long as one is dealing with frequencies much less than the plasma frequency ω_p. For frequencies comparable to ω_p only a dynamical local field can provide an adequate description of the system response. As in the 3D case it is essential to include a dynamical local field $G(k,\omega)$ if one were to understand the excitation spectrum $S(k,\omega)$ of the 2D electron liquid. A microscopic theory of dynamical correlations which is physically transparent and at the same time mathematically tractable is by no means an easy task. As a first step in this direction we wish to calculate in this paper the contribution of the three first-order Feynman diagrams to the proper polarizability for arbitrary wave vector and frequency. As we shall see, this in itself is a fairly involved calculation. An analo-

gous calculation in the 3D case was done recently by Holas *et al.*[6]

The plan of the paper is as follows. In Sec. II we introduce our notation and write down the expressions for the zeroth- and first-order polarizabilities. The behavior of the dimensionless polarizibility is examined in Sec. III and the dynamical local field $G(k,\omega)$ is introduced in Sec. IV. We evaluate the plasmon dispersion and examine the high- and low-frequency behavior of $Q^1(k,\omega)$ and the sum rules in Sec. V. In Sec. VI we examine the behavior of the dynamic and static structure factors and the static pair correlation function. Relevant details of the calculations are given in the Appendices.

II. FIRST-ORDER DIAGRAMS FOR THE PROPER POLARIZABILITY

The lowest-order diagrams for the proper polarizability $\pi(k)$ are shown in Fig. 1. The zeroth-order contribution $\pi^0(k)$ is

$$\pi^0(k)=\frac{2}{\hbar}\int\frac{d^3p}{(2\pi)^3 i}G^0(p)G^0(p+k)\ , \tag{2.1}$$

where p is the 2D counterpart of the 3D 4-vectors

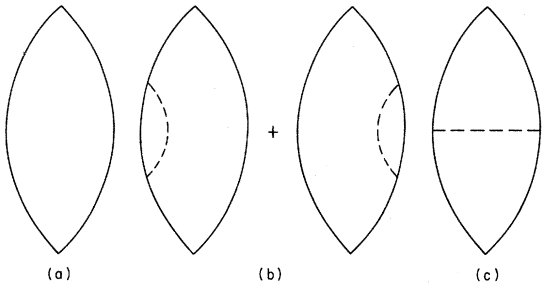

FIG. 1. Diagrams for proper polarizability: (a) the zeroth-order and (b) the first-order self-energy part; (c) the first-order exchange part.

with $p=(\vec{p},p_0)$ and $k=(\vec{k},\omega)$. $G^0(p)$ is the free-particle Green's function,

$$G^0(p)=\frac{1}{p_0-\omega_{\vec{p}}-i\eta\,\mathrm{sgn}(k_F-|\vec{p}|)}\ ,\quad \eta=0^+ \tag{2.2}$$

where $\omega_{\vec{p}}=\hbar\vec{p}^2/2m$ and k_F is the Fermi wave vector.

The first-order diagrams contribute the self-energy part π^{SE} and the exchange-energy part π^{ex}:

$$\pi^{SE}(k)=\frac{2}{\hbar}\int\frac{d^3p}{(2\pi)^3 i}G^0(p)G^0(p+k)[\Sigma^0(p)G^0(p)+\Sigma^0(p+k)G^0(p+k)]\ , \tag{2.3}$$

where

$$\Sigma^0(p)=\frac{-1}{\hbar}\int\frac{d^3p'}{(2\pi)^3 i}v(\vec{p}'-\vec{p})G^0(p')e^{ip_0'\eta} \tag{2.4}$$

and

$$\pi^{ex}(k)=\frac{-2}{\hbar^2}\int\frac{d^3p}{(2\pi)^3 i}\frac{d^3p'}{(2\pi)^3 i}G^0(p)G^0(p+k)v(\vec{p}-\vec{p}')G^0(p')G^0(p'+k)\ . \tag{2.5}$$

$v(\vec{p})=2\pi e^2/|\vec{p}|$ is the 2D Fourier transform of the electron-electron interaction potential.

The frequency integrals in (2.1) and (2.3)–(2.5) can be done by contour integration. We define the dimensionless polarizability by

$$Q(\vec{k},\omega)=-v(\vec{k})\pi(\vec{k},\omega) \tag{2.6}$$

and measure wave vectors in units of k_F and frequency in units of $2E_F/\hbar$. After simplification, the zeroth-order contribution (RPA) can be written as

$$\mathrm{Re}Q^0(\vec{k},\omega)=\frac{2\pi\alpha_D}{k^2}[k+\mathrm{sgn}(\nu_+)\Theta(\nu_+^2-1)(\nu_+^2-1)^{1/2}+\mathrm{sgn}(\nu_-)\Theta(\nu_-^2-1)(\nu_-^2-1)^{1/2}] \tag{2.7a}$$

and

$$\mathrm{Im}Q^0(\vec{k},\omega)=\frac{2\pi\alpha_D}{k^2}[\Theta(1-\nu_+^2)(1-\nu_+^2)^{1/2}-\Theta(1-\nu_-^2)(1-\nu_-^2)^{1/2}]\ , \tag{2.7b}$$

where $\alpha_D = r_s/\sqrt{2}\pi$,

$$\nu_\pm = \pm\frac{\omega}{k} - \frac{k}{2} , \tag{2.8}$$

and

$$\Theta(x) = \begin{cases} 1, & x > 0 \\ 0, & x < 0 . \end{cases}$$

The first-order contribution can be written as

$$Q^1(\vec{k},\omega) = \frac{\alpha_D^2}{k}[F^{\mathrm{SE}}(\vec{k},\omega) + F^{\mathrm{ex}}(\vec{k},\omega)] ,$$

where

$$F^{\mathrm{SE}}(\vec{k},\omega) = -\tfrac{1}{2}\int \frac{d^2p\, d^2p'}{|\vec{p}-\vec{p}'|} \frac{(n^0_{\vec{p}} - n^0_{\vec{p}+\vec{k}})(n^0_{\vec{p}'} - n^0_{\vec{p}'+\vec{k}})}{(\omega + \omega_{\vec{p}} - \omega_{\vec{p}+\vec{k}} + i\eta)^2} , \tag{2.9}$$

$$F^{\mathrm{ex}}(\vec{k},\omega) = \tfrac{1}{2}\int \frac{d^2p\, d^2p'}{|\vec{p}-\vec{p}'|} \frac{(n^0_{\vec{p}} - n^0_{\vec{p}+\vec{k}})(n^0_{\vec{p}'} - n^0_{\vec{p}'+\vec{k}})}{(\omega + \omega_{\vec{p}} - \omega_{\vec{p}+\vec{k}} + i\eta)(\omega + \omega_{\vec{p}'} - \omega_{\vec{p}'+\vec{k}} + i\eta)} , \tag{2.10}$$

and

$$\omega_{\vec{p}} = \tfrac{1}{2}p^2, \quad n^0_{\vec{p}} = \Theta(1-\vec{p}^2) .$$

The functions F^{SE} and F^{ex} are complex. $\mathrm{Im}Q^1$ is evaluated first and $\mathrm{Re}Q^1$ is then obtained by taking the Hilbert transform. The result is

$$\mathrm{Im}Q^1(\vec{k},\omega) = \frac{\alpha_D^2}{k}[\Theta(1-\nu_+^2)\phi(k,\nu_+) - \Theta(1-\nu_-^2)\phi(k,\nu_-)] , \tag{2.11}$$

where

$$\phi(k,\nu) = \phi^{\mathrm{SE}}(k,\nu) + \phi^{\mathrm{ex}}(k,\nu) . \tag{2.12}$$

For the details of the evaluation of $\mathrm{Im}Q^1$ see Appendices A and B.

It can be seen from (2.7) and (2.11) that $\mathrm{Im}Q^0$ and $\mathrm{Im}Q^1$ are nonzero in the ω-k plane where at least one of the Θ functions is nonzero [the region of the electron-hole (*e-h*) excitation]. This region is bounded by the lines $\nu_\pm^2 = 1$ (*e-h* edges) as shown in Fig. 2. $Q^1(k,\omega)$ is singular at the *e-h* edges, except $Q^1(2,\omega)$, which has a spike of finite height. $Q^0(k,\omega)$ has cusps at the *e-h* edges.

The integrals in $\phi^{\mathrm{SE}}(k,\nu)$ and $\phi^{\mathrm{ex}}(k,\nu)$ are calculated numerically [see Eqs. (A15) and (B12)] with care taken to accurately account for the contributions from the unpleasant but integrable singularities in the integrands. $Q^1(k,\omega)$ is analytic in the complex upper-half ω plane. This and the fact that the $\mathrm{Re}Q^1$ varies as ω^{-4} for large ω justifies the use of the Hilbert transform to numerically calculate $\mathrm{Re}Q^1$ from $\mathrm{Im}Q^1$,

$$\mathrm{Re}Q^1(\vec{k},\omega) = \frac{1}{\pi}\int_{-\infty}^{+\infty} \frac{\mathrm{Im}Q^1(\vec{k},\omega')}{(\omega'-\omega)} d\omega' . \tag{2.13}$$

III. BEHAVIOR OF THE FUNCTION $Q^1(\vec{k},\omega)$

$\mathrm{Im}Q^1$ and $\mathrm{Re}Q^1$ as functions of ω show many qualitative similarities with the corresponding functions in the 3D case.[6] However, the nature of the singularities is different. The singularities occur at the frequencies ω_s^-, ω_s^+ (Fig. 2), and $\omega = 0$ is an interesting point. The behavior of these functions about these points is summarized below:

(a) For $k < 2$

$$\mathrm{Im}Q^1 \rightarrow \begin{cases} \omega \ln\omega, & \omega \rightarrow 0+ \\ \dfrac{\alpha}{\sqrt{x}} + \beta\sqrt{x} + \gamma\sqrt{x}\,\ln x, & x = (\omega_s^{\pm} - \omega) \rightarrow 0+ \\ \alpha'\sqrt{x} + \beta'\sqrt{x}\,\ln x, & x = (\omega - \omega_s^{-}) \rightarrow 0+ \; . \end{cases}$$

(b) For $k > 2$

$$\mathrm{Im}Q^1 \rightarrow \frac{\alpha}{\sqrt{x}} + \beta\sqrt{x} + \gamma\sqrt{x}\,\ln x \quad \text{for } x = (\omega_s^{+} - \omega) \rightarrow 0+ \text{ or } x = (\omega - \omega_s^{-}) \rightarrow 0+ \; .$$

The most prominant singularity is of the type $1/\sqrt{x}$, which produces a similar singularity in $\mathrm{Re}Q^1(\vec{k},\omega)$. $\mathrm{Re}Q^1$ also has the $\ln x$ type of singularity. Q^1 and Q^0 for $k=1$ and $r_s=0.5$ are shown in Fig. 3. Even at this relatively high density, the Q^1 contribution is quite large compared to Q^0. The singular portions of the plots close to $\omega_s^{\pm}$ are omitted, because as discussed in Ref. 6 perturbation theory cannot be trusted in this region.

For $k=2$, there is a cancellation of the singularities of $\mathrm{Im}Q^1$ close to $\omega=0$, which makes the function finite but with very large slope. This produces a sharp finite spike in $\mathrm{Re}Q^1$ at $\omega=0$ (Fig. 4). This effect is due to the finite-order perturbation theory.

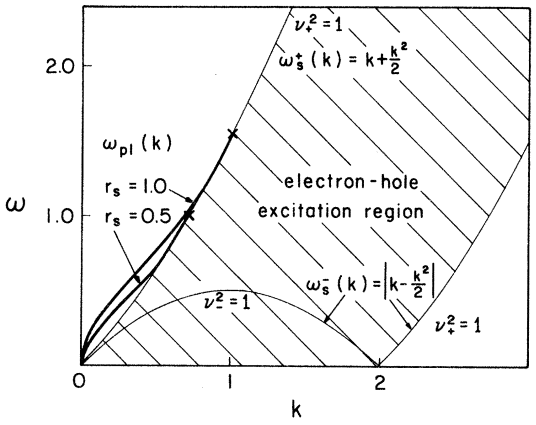

FIG. 2. The electron-hole excitation region and the *e-h* edges $\omega_s^{\pm}(k)$. The first-order polarizability $Q^1(\vec{k},\omega)$ is singular at $\omega_s^{\pm}(k)$ except at $k=2$ and $\omega=0$. Both $\mathrm{Im}Q^1$ and $\mathrm{Im}Q^0$ are nonzero only within the *e-h* excitation region (shaded region). The RPA plasmon dispersion curves (thick lines) $\omega_{pl}^0(k)$ in relation to the *e-h* edges for $r_s=0.5$ and 1.0 are shown. The cross on $\omega_s^+(k)$ is at k_c given by Eq. (5.8). ω is in units of $2E_F/h$ and k is in units of k_F (here and elsewhere).

IV. THE DYNAMIC LOCAL FIELD $G(\vec{k},\omega)$

The dielectric function is defined as

$$\epsilon(\vec{k},\omega) = 1 + Q(\vec{k},\omega) \; . \tag{4.1}$$

The defining equation for the local field G is

$$\epsilon(\vec{k},\omega) = 1 + \frac{Q^0(\vec{k},\omega)}{1 - G(\vec{k},\omega)Q^0(\vec{k},\omega)} \; . \tag{4.2}$$

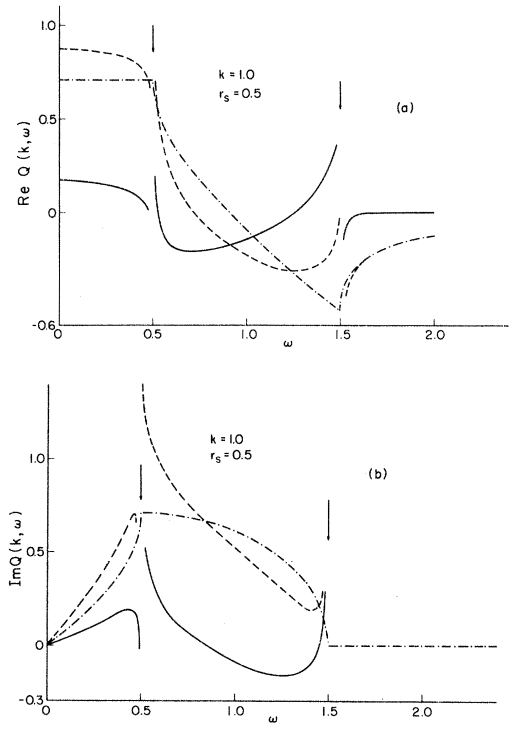

FIG. 3. The dimensionless polarizability $Q(\vec{k},\omega)$ vs ω at $k=1.0$, $r_s=0.5$. $-\cdot-\cdot-\cdot-$ $Q^0(\vec{k},\omega)$, —— $Q^1(\vec{k},\omega)$, and – – – – $Q^0(\vec{k},\omega)+Q^1(\vec{k},\omega)$. The arrows point to the singularities of Q^1 at $\omega_s^{\pm}$. (a) Real part; (b) imaginary part.

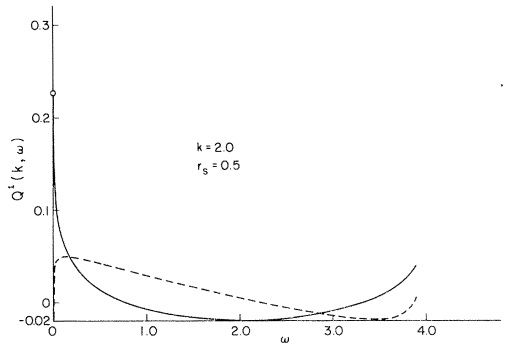

FIG. 4. Dimensionless polarizability $Q^1(k,\omega)$ vs ω at $k=2.0$ and $r_s=0.5$. For $\omega=0$, $\mathrm{Re}Q^1$ has a finite spike. —— $\mathrm{Re}Q^1$, – – – – – $\mathrm{Im}Q^1$.

In the RPA $G=0$. In the present approximation $Q=Q^0+Q^1$, and therefore

$$G(\vec{k},\omega)=\frac{Q^1(\vec{k},\omega)}{Q^0(\vec{k},\omega)[Q^0(\vec{k},\omega)+Q^1(\vec{k},\omega)]} . \tag{4.3}$$

Both ReG and ImG as functions of ω have a qualitative similarity to the corresponding functions in the 3D case.[6] ReG and ImG are plotted in Fig. 5 for $k=1.0$ and $r_s=0$, 0.25, 0.5, and 1.0. ReG varies strongly and attains a maximum close to the upper e-h edge, drops sharply to negative values, and finally approaches the (positive) asymptotic value. ImG is very small in the $(0,\omega_s^-)$ range, varies strongly in the (ω_s^-,ω_s^+) region, and is zero for $\omega>\omega_s^+$ or for $\omega<\omega_s^-$ and $k>2$.

The static local field divided by k, $G(k,0)/k$, is shown in Fig. 6. The peak at $k=2$ is due to a similar peak in $Q^1(k,0)$. The origin of this peak was explained in Sec. III. In the limit $k\to 0$, Q^0 and $Q^1\to k^{-1}$ and in the limit $k\to\infty$, $Q^0=2\sqrt{2}r_s/k^3$, and $Q^1=4r_s^2/k^6$. Thus

$$\lim_{k\to 0} G(k,0)\to 0 ,$$

and

$$\lim_{k\to\infty} G(k,0)\to\tfrac{1}{2} .$$

This leads to a considerable change in screening at small distances as compared to the RPA. The undamped plasmons in the present approximation can be traced to the absence of the long-wavelength tail of Im$G(\vec{k},\omega)$.

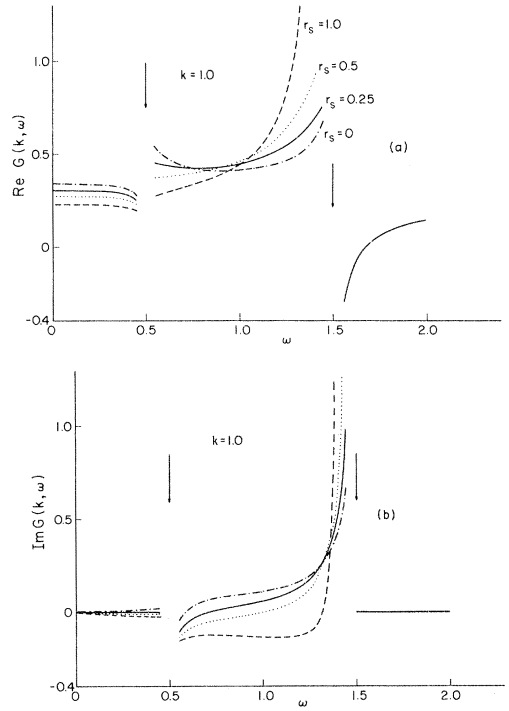

FIG. 5. The dynamic local field $G(\vec{k},\omega)$ vs ω for $k=1.0$. $-\cdot-\cdot-$ $r_s=0$, —— $r_s=0.25$, ····· $r_s=0.5$, —— $r_s=1.0$. The arrows point to the singular points of G. (a) Real part; (b) imaginary part.

V. PLASMON DISPERSION, HIGH- AND LOW-FREQUENCY BEHAVIOR OF $Q^1(\vec{k},\omega)$, AND SUM RULES

In the RPA, the dielectric function is

$$\epsilon(\vec{k},\omega)=1+Q^0(\vec{k},\omega) . \tag{5.1}$$

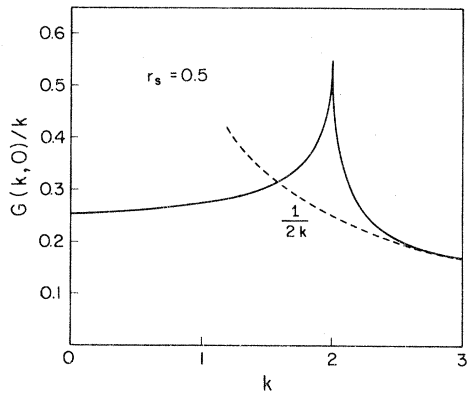

FIG. 6. Static local field $G(k,0)$ divided by k vs k for $r_s=0.5$. The dashed curve shows the asymptotic behavior of the function. The spike at $k=2.0$ is reminiscent of a similar spike in $\pi^1(k,0)$.

The condition for the existence of the plasma oscillations is

$$\epsilon(\vec{k},\omega)=0\ , \tag{5.2}$$

which leads to

$$1+\mathrm{Re}Q^0(\vec{k},\omega)=0\ , \tag{5.3a}$$

$$\mathrm{Im}Q^0(\vec{k},\omega)=0\ . \tag{5.3b}$$

For $\omega>\omega_s^+$ $[\omega_s^+=(k+k^2/2)]$, $\mathrm{Im}Q^0(\vec{k},\omega)=0$, and thus the condition (5.2) reduces to

$$(\nu_+^2-1)^{1/2}-(\nu_-^2-1)^{1/2}=-k(Bk+1)\ , \tag{5.4}$$

where $B=1/2\pi\alpha_D$.

Equation (5.4) gives the following RPA plasmon dispersion relation:

$$[\omega_{\mathrm{pl}}^0(k)]^2=\frac{k}{2B}\frac{(1+Bk)^2(1+\frac{1}{2}Bk^3+\frac{1}{4}B^2k^4)}{1+\frac{1}{2}Bk}\ . \tag{5.5}$$

Such a closed expression for $\omega_{\mathrm{pl}}^0(k)$, as far as we are aware, has not been given in earlier papers.[4,7,8] The leading term in the long-wavelength expansion $(k\to 0)$ of (5.5) is

$$\omega_p^2(k)=\frac{r_s k}{\sqrt{2}}\ . \tag{5.6}$$

The condition for the existence of undamped plasma oscillations, $\omega_{\mathrm{pl}}>\omega_s^+$, is satisfied for small k and finite r_s and is valid up to a certain $k=k_c$. At this wave vector

$$\Delta\omega^2(k)\equiv[\omega_{\mathrm{pl}}^0(k)]^2-[\omega_s^+(k)]^2=0\ . \tag{5.7}$$

Solving this we get the equation

$$\frac{k_c^2}{\sqrt{2}r_s}+\frac{k_c^3}{4r_s^2}=1\ . \tag{5.8}$$

Introducing the function

$$R(x)=\left[\frac{x^2}{\sqrt{2}}+\frac{x^3}{4}\right]^{-1}\ , \tag{5.9}$$

condition (5.8) becomes

$$R(x)=r_s\ , \tag{5.10}$$

where $x=k_c/r_s$.

The root of Eq. (5.10) gives k_c; there is only one such root. For example, $k_c=1.02$, 0.74, and 0.27 for $r_s=1.0$, 0.5, and 0.1, respectively. The function $\Delta\omega^2(k)$ approaches the k axis parabolically, hence the plasmon and e-h lines do not intersect, but are tangential at k_c. For $k>k_c$, Eq. (5.2) has no solution. The plots of (5.5) are shown in Fig. 2.

In the first-order theory, the dispersion relation cannot be expressed in a closed form; nonetheless the long-wavelength form can be evaluated. The long-wavelength expansions of $\mathrm{Re}Q^0$ and $\mathrm{Re}Q^1$ are

$$\mathrm{Re}Q^0(\vec{k},\omega)=\frac{-r_s k}{\sqrt{2}\omega^2}\left[1+\frac{3}{4}\frac{k^2}{\omega^2}+O(k^4)\right]\ , \tag{5.11}$$

$$\mathrm{Re}Q^1(\vec{k},\omega)=\frac{5r_s^2}{12\pi}\frac{k^3}{\omega^4}+O(k^4)\ . \tag{5.12}$$

The plasmon dispersion relation is found by solving

$$\epsilon(\vec{k},\omega)=1+Q^0(\vec{k},\omega)+Q^1(\vec{k},\omega)=0\ . \tag{5.13}$$

We thus obtain

$$[\omega_{\mathrm{pl}}(k)]^2=\omega_p^2(k)[1+Pk+O(k^2)]\ , \tag{5.14a}$$

where

$$P=\frac{3\sqrt{2}}{4r_s}\left[1-\frac{10}{9\sqrt{2}\pi}r_s\right]\ . \tag{5.14b}$$

Equation (5.14a) is the same as obtained by Rajagopal.[2] The second term in (5.14b) is the first-order correction to the RPA and its value is very small for $r_s<1$, i.e., in the range of validity of the present perturbation result.

Before discussing the behavior of $Q^1(\vec{k},\omega)$ for arbitrary k and ω, we consider its behavior for high and low frequencies. For ω greater than that of the e-h edge in Fig. 2, $\mathrm{Im}Q^1(\vec{k},\omega)=0$; therefore $i\eta$ may be omitted in the denominators in (2.9) and (2.10). For large ω, $Q^1(\vec{k},\omega)$ can be expressed as

$$Q^1(\vec{k},\omega)\simeq\frac{-\alpha_D^2}{4k\omega^4}\int\frac{d^2p\,d^2p'}{|\vec{p}-\vec{p}'|}(n^0_{\vec{p}}-n^0_{\vec{p}+\vec{k}})(n^0_{\vec{p}'}-n^0_{\vec{p}'+\vec{k}})[(\vec{p}'-\vec{p})\cdot\vec{k}]^2=\left[\frac{\omega_p(k)}{\omega}\right]^4 G^{\infty}_{\mathrm{HF}}(\vec{k})\ , \tag{5.15}$$

where $G^{\infty}_{\mathrm{HF}}(k)$, analogous to the 3D case, is

$$G^{\infty}_{\mathrm{HF}}(\vec{k})=\frac{1}{2\pi k^3}\int d^2q\frac{(\vec{k}\cdot\vec{q})^2}{q}[S_{\mathrm{HF}}(q)-S_{\mathrm{HF}}(|\vec{k}+\vec{q}|)]\ , \tag{5.16}$$

and

$$S_{\mathrm{HF}}(q)=\frac{1}{\pi}\int d^2p\, n^0_{\vec{p}}(1-n^0_{\vec{p}+\vec{q}})=\begin{cases}\dfrac{2}{\pi}\left\{\sin^{-1}\left[\dfrac{q}{2}\right]+\dfrac{q}{2}\left[1-\left[\dfrac{q}{2}\right]^2\right]^{1/2}\right\}, & q<2\\ 1, & q>2\end{cases} \tag{5.17}$$

is the Hartree-Fock (HF) structure factor for the 2D electron gas.[9] One of the two integrations in (5.16) can be done analytically (Appendix C) and we get

$$G^{\infty}_{\mathrm{HF}}(k)=\frac{1}{2\pi k}\int_0^{\infty} dq\, q[1-S_{\mathrm{HF}}(q)][Z(q,k)-\pi q]\ , \tag{5.18}$$

where

$$Z(q,k)=\frac{2}{3}\frac{(k+q)}{k^2}[K(\tilde{q})(q-k)^2 +E(\tilde{q})(5k^2-q^2)]\ , \tag{5.19}$$

and

$$\tilde{q}=\left[\frac{4qk}{(q+k)^2}\right]^{1/2}.$$

In the limit $k\to 0$, the remaining integration can be done analytically and we obtain

$$G^{\infty}_{\mathrm{HF}}(k)=\frac{5}{6\pi}k+O(k^2) \tag{5.20}$$

and $Q^1(k,\omega)$ is given by (5.12). For arbitrary k, the integration has to be done numerically.

Now expand the right-hand side (rhs) of the dispersion relation (2.19) for large ω and compare it with the left-hand side (lhs). Since $\mathrm{Im}Q^1(k,\omega)$ is an odd function of ω, the even moments are zero. Using (5.15), the first and third moments are

$$\langle\omega\rangle_{\mathrm{Im}Q^1}\equiv\int_0^{\infty} d\omega\,\omega\,\mathrm{Im}Q^1(k,\omega)=0\ , \tag{5.21a}$$

$$\langle\omega^2\rangle_{\mathrm{Im}Q^1}\equiv\int_0^{\infty} d\omega\,\omega^3\,\mathrm{Im}Q^1(k,\omega) =-\frac{\pi}{2}\omega_p^4(k)G^{\infty}_{\mathrm{HF}}(k)\ . \tag{5.21b}$$

For small k, $\langle\omega^3\rangle_{\mathrm{Im}Q^1}=-\frac{5}{24}k^3r_s^2$. Figure 7 shows the plot of the third moment versus k for $r_s=1.0$. The accuracy of the numerical results of $\mathrm{Im}Q^1$ was tested by (5.21). To check whether (5.21a) is satisfied, the first moment values were divided by the values of the analogous integral of the absolute value of $\mathrm{Im}Q^1$; for all wave vectors of interest the quotients were less than 10^{-4}. The third-moment sum rule was satisfied to an accuracy better than 0.1%.

The density-density response function is given by

$$\chi(k,\omega)=\frac{-1}{v(k)}\frac{Q(\vec{k},\omega)}{1+Q(\vec{k},\omega)}\ . \tag{5.22}$$

The asymptotic expansion of this is

$$-v(k)\chi(\vec{k},\omega)=\frac{M_1}{\omega^2}+\frac{M_3}{\omega^4}+O(1/\omega^6)\ , \tag{5.23}$$

where

$$M_1=\frac{v(\vec{k})}{\pi}\int_{-\infty}^{\infty} d\omega'\omega'\,\mathrm{Im}\chi(\vec{k},\omega')=\omega_p^2(k) \tag{5.24}$$

and

$$M_3=\frac{v(\vec{k})}{\pi}\int_{-\infty}^{\infty} d\omega'\omega'^3\,\mathrm{Im}\chi(\vec{k},\omega') =-\omega_p^2(k)\left[\frac{k^4}{4}+\tfrac{3}{2}k^2\frac{\langle E_{\mathrm{kin}}\rangle}{E_F} +\omega_p^2(k)[1-G^{\infty}(k)]\right], \tag{5.25}$$

where $\omega_p^2(k)$ is given by (5.6). $\langle E_{\mathrm{kin}}\rangle$ is the average kinetic energy per particle of the interacting electron gas, and $G^{\infty}(k)$ is given by (5.16) with

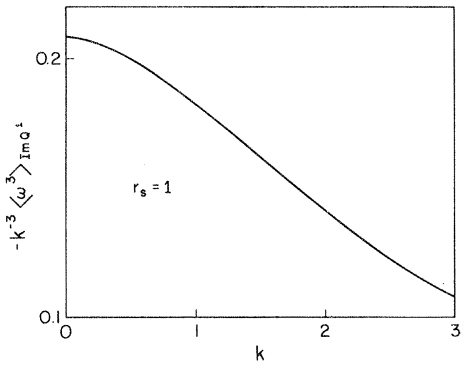

FIG. 7. Third moment of $\mathrm{Im}Q^1(\vec{k},\omega)$ times $(-k^{-3})$ vs k for $r_s=1.0$.

$S_{\rm HF}(q)$ replaced by the true structure factor $S(q)$. The derivation of the first moment is the same as in the 3D case,[10] but in the derivation of the third moment the 2D nature of the system manifests itself. While evaluating the commutators in $\langle\omega^3\rangle$ (see Ref. 10) one averages over the angles; here $\langle\cos^2\theta\rangle_{2D}=\frac{1}{2}$, while $\langle\cos^2\theta\rangle_{3D}=\frac{1}{3}$. This is the origin of the factor $\frac{3}{2}$ in the second term in (5.25).

In the present approximation the density-density response function is

$$\chi^1(\vec{k},\omega)=\frac{-1}{v(k)}\frac{Q^0(\vec{k},\omega)+Q^1(\vec{k},\omega)}{1+Q^0(\vec{k},\omega)+Q^1(\vec{k},\omega)} . \tag{5.26}$$

Expanding this for large ω and comparing the moments with the exact ones, one finds,

$$M_1^{(1)}=M_1,\quad M_3^{(1)}\neq M_3 ,$$

where

$$M_3^{(1)}=-\omega_p^2(k)\{\tfrac{1}{4}k^4+\tfrac{3}{4}k^2+\omega_p^2(k)[1-G_{\rm HF}^{\infty}(k)]\} . \tag{5.27}$$

This differs from M_3 in having the average kinetic energy of the noninteracting gas $\frac{1}{2}E_F$ instead of $\langle E_{\rm kin}\rangle$ and $G_{\rm HF}^{\infty}(k)$ instead of $G^{\infty}(k)$.

Let us consider the static $Q^1(k,\omega)$. $\mathrm{Im}Q^1(k,\omega)$ being an odd function of ω is zero at $\omega=0$ and $Q^1(k,0)$ is given by

$$Q^1(k,0)=\frac{-\alpha_D^2}{4k}\int\frac{d^2p\,d^2p'}{|\vec{p}-\vec{p}'|}\frac{(n^0_{\vec{p}}-n^0_{\vec{p}+\vec{k}})(n^0_{\vec{p}'}-n^0_{\vec{p}'+\vec{k}})}{[k^2/2+\vec{p}\cdot\vec{k}]^2[k^2/2+\vec{p}'\cdot\vec{k}]^2}[(\vec{p}-\vec{p}')\cdot\vec{k}]^2 . \tag{5.28}$$

It is more convenient to work in terms of proper polarizability $\pi(k)$, defined by (2.6). In the long-wavelength limit ($k\to 0$), $Q^1(k,0)$ can be evaluated analytically and we have

$$\pi^1(0,0)=\frac{-m\sqrt{2}r_s}{\hbar^2\pi^2} . \tag{5.29}$$

Also in the small-wavelength limit ($k\to\infty$), $Q^1(\vec{k},0)$ can be evaluated and we obtain

$$\lim_{k\to\infty}[Q^1(\vec{k},0)k^6]=4r_s^2 . \tag{5.30}$$

For arbitrary k, the integrations in (5.28) have to be done numerically. To maintain the symmetric structure of the integrand, no partial and analytic integration is attempted; instead some ideas of Geldart and Taylor[11] are exploited to transform (5.28) into a four-dimensional integral over the unit cube. The singularities of the integrand are practically removed, so that exact numerical integration is possible. The results in the limiting cases agree with (5.29) and (5.30) to a high accuracy. This rather complex integration process has been outlined in detail in Ref. 12. The values obtained are close to those given by Maldague,[13] with some quantitative differences. We get $\pi^1(2,0)/\pi^1(0,0)=2.832$ instead of 2.5 obtained by Maldague, and

$$\pi^0(2,0)+\pi^1(2,0)=-\frac{m}{\hbar^2}(0.32+0.41r_s) . \tag{5.31}$$

The plot of $\pi^1(k,0)/\pi^1(0,0)$ versus k is given in Fig. 8.

In the "linearized vertex function formalism" of Rajagopal, Eq. (3) of Ref. 2 can be solved exactly in this approximation and we have found that

$$\pi(0,0)=\frac{-m}{\pi\hbar^2}\frac{1}{1-(\sqrt{2}/\pi)r_s}$$
$$\simeq\frac{-m}{\hbar^2\pi}-\frac{m\sqrt{2}r_s}{\pi^2\hbar^2}=\pi^0+\pi^1 \tag{5.32}$$

for $r_s<<1$. There is a difference of a minus sign in the definition of π between Rajagopal's and ours. Our result (5.29) coincides with (5.32) for $r_s<<1$. The polarizability π of (5.32) diverges for $r_s=\pi/\sqrt{2}=2.22$, which may be interpreted as the radius of convergence of the perturbation expansion, or one may speculate about the instability of the system for low densities.

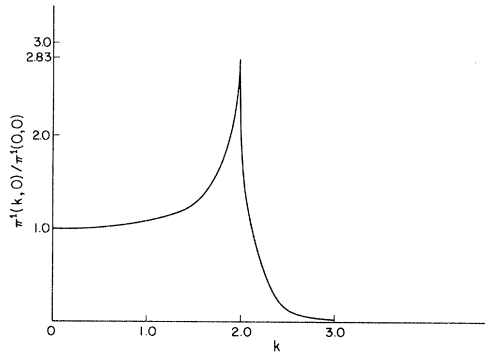

FIG. 8. The ratio $\pi^1(\vec{k},0)/\pi^1(0,0)$ vs k. Note the spike at $k=2.0$.

VI. DYNAMIC AND STATIC STRUCTURE FACTORS, SUM RULES, AND PAIR CORRELATION FUNCTION

The differential inelastic-scattering cross section for x rays and electrons is proportional to the dynamic structure factor $S(\vec{k},\omega)$. The fluctuation dissipation theorem in the 2D case is[14]

$$S(\vec{k},\omega)=\frac{1}{\pi v(k)}\,\mathrm{Im}\left[\frac{-1}{\epsilon(\vec{k},\omega)}\right]. \tag{6.1}$$

$S(\vec{k},\omega)$ has qualitative similarity with that in the 3D case,[6] especially for large k's. Our calculated values of $S(\vec{k},\omega)$ are plotted as a function of ω for $k=1.0$, $r_s=0.5$, in different approximations in Fig. 9. The peak position ($\omega=1.1$) in the present approximation [first order (FO)] occurs at a much lower frequency compared to that in the RPA ($\omega=1.4$); and the free-electron peak [Hartree-Fock approximation (HFA)] occurs at a still lower frequency ($\omega=0.5$). $S(k,\omega)$ is more symmetric in first order than in RPA or HFA.

The peak positions of $S(k,\omega)$ for various momentum transfers in the different approximations are plotted in Fig. 10 for $r_s=0.5$. For $k<k_c$ (point marked by a cross on the ω_s^+ curve), both the plasmons and the electron-hole excitations contribute to the total intensity. The plasmons predominate for $k<0.5$ and the electron-hole excitations predominate for $k>0.5$. For $k>k_c$ only the electron-hole excitations contribute. The FO and RPA plasmon curves are almost indistinguishable in the present case. The FO peak always lies between the RPA and free-electron peaks.

Let us consider the sum rules of $S(\vec{k},\omega)$. The first-moment sum rule is

$$\langle\omega\rangle_s\equiv\int_0^\infty d\omega\,\omega S(\vec{k},\omega)=\frac{Nk^2}{2m}, \tag{6.2}$$

where N is the number of electrons per unit area,

$$\langle\omega^{-1}\rangle_s\equiv\int_0^\infty\frac{d\omega}{\omega}S(\vec{k},\omega)=\frac{-1}{2}\chi(k,0)=\frac{1}{2v(k)}\frac{Q(k,0)}{\epsilon(k,0)}. \tag{6.3}$$

In the limit of long wavelength

$$\lim_{k\to0}\langle\omega^{-1}\rangle_s=\frac{1}{2v(k)},$$

and

$$\lim_{k\to0}\frac{\langle\omega\rangle_s}{\langle\omega^{-1}\rangle_s}=\omega_p^2(k).$$

The sum rules (6.2) and (6.3) are useful as checks of the numerical results of Q^1. The static structure factor is defined by

$$S(\vec{k})=\frac{\hbar}{N}\int_0^\infty S(\vec{k},\omega)d\omega. \tag{6.4}$$

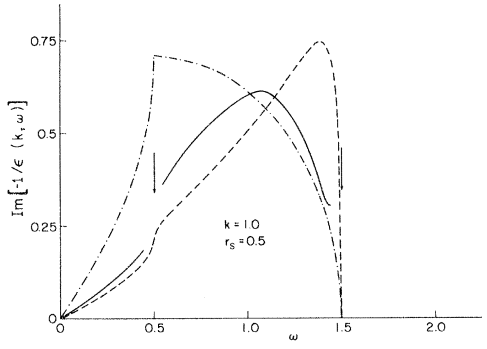

FIG. 9. Energy loss function $\mathrm{Im}[-1/\epsilon(\vec{k},\omega)]$ vs ω for $k=1.0$ and $r_s=0.5$; ·—·—·— free-electron gas; – – – – – RPA; —— present approximation.

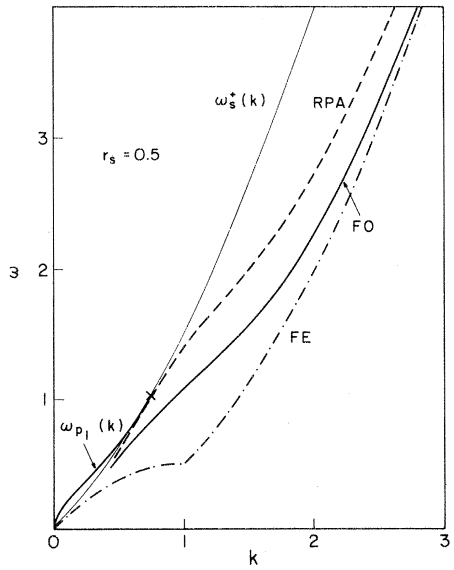

FIG. 10. Plasmon dispersion curve $\omega_{\mathrm{pl}}(k)$ and peak positions of $S(\vec{k},\omega)$ for $r_s=0.5$. The RPA and first-order plasmon dispersion curves are the same within the accuracy of the figure. The cross on $\omega_s^+(k)$ is at k_c. Peak positions of $S(k,\omega)$ ·—·—·— in the free-electron gas, – – – – – in the RPA, —— in first-order theory. About $k=0.5$ the plasmon and the electron-hole contributions to $S(k)$ are nearly the same.

In the long-wavelength limit it is reasonable to assume that the major contribution to $S(\vec{k},\omega)$ is from the plasmons.[15] In that case the form of the structure factor $S_{\rm pl}(\vec{k},\omega)$ is

$$S_{\rm pl}(\vec{k},\omega)=\frac{1}{\hbar}NA_k\delta(\omega-\omega_k)\ . \tag{6.5}$$

Using the sum rules (6.2) and (6.3) in the $k\to 0$ limit, we obtain

$$\omega_k=\omega_p(k) \tag{6.6}$$

and

$$A_K=\frac{\hbar k^2}{2m\omega_p(k)}\ .$$

Using $\omega_p(k)$ of (5.6) we have

$$A_k=2^{-3/4}r_s^{-1/2}k^{3/2}\ . \tag{6.7}$$

Using the $\epsilon(\vec{k},\omega)$ of RPA in (6.1) and (6.4), the e-h contribution is found to be $S^0_{e\text{-}h}(k)=(3\pi r_s^2)^{-1}k^3$ and using the $\epsilon(k,\omega)$ of FO, $S^1_{e\text{-}h}(k)\sim k^3$ in the long-wavelength limit. This justifies the assumption made above.

In the small-wavelength limit, according to Ref. 4,

$$\lim_{k\to\infty}S(k)\simeq 1+\frac{C}{k^3}\ . \tag{6.8}$$

Using (4.1) and (6.1) in (6.4) we find C to be

$$C=\lim_{k\to\infty}\left\{k^3\left[\frac{\sqrt{2}}{\pi}\frac{k}{r_s}\int_0^\infty d\omega\,\mathrm{Im}\left[-\frac{1}{1+Q(k,\omega)}\right]-1\right]\right\}. \tag{6.9}$$

The above integration can be done in this limit (Appendix D) and we get

$$C=\sqrt{2}r_s[-1+\tfrac{1}{2}]\ , \tag{6.10}$$

where the first term in the square bracket is the RPA contribution, and the second term is from FO, similar to the 3D case.

For intermediate values of k, $S(k)$ is calculated numerically and the result is shown in Fig. 11. The values of $S(k)$ in the present approximation lie between the HFA and RPA values.

The pair correlation function $g(r)$ is given by

$$g(r)=1+\int_0^\infty dk\,kJ_0(kr)[S(k)-1]\ , \tag{6.11}$$

where r is in units of k_F^{-1} and $J_0(kr)$ is the Bessel function of the first kind of order zero. At $r=0$

$$g(0)=1+\int_0^\infty dk\,k[S(k)-1]\ . \tag{6.12}$$

The integration is done numerically and Fig. 12 shows $g(0)$ as a function of r_s. The region where $g(0)>0$ in the first-order approximation is almost double that in the RPA. The Hubbard and STLS approximations seem to be even better.[3]

Using the large-k expansion of $S(k)$ [Eq. (6.8)] in (6.11) we find that[4]

$$\left|\frac{dg(r)}{dr}\right|_{r\to 0}=-C\ . \tag{6.13}$$

This is similar to the corresponding relation in the 3D case.[16] The only assumption used in the derivation of (6.13) is the asymptotic behavior of $S(k)$ given by (6.8). Therefore (6.13) must be satisfied by an approximate theory and is a good check of the numerical calculation of $g(0)$. It is fulfilled

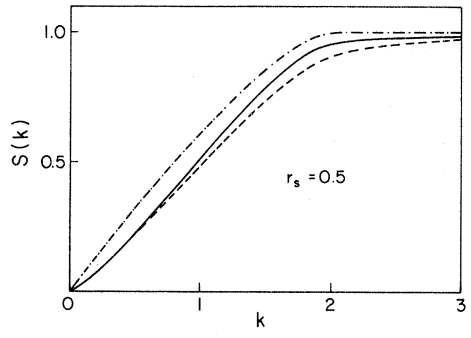

FIG. 11. Static structure factor $S(k)$ vs k: ·—·—· free-electron gas, – – – – – RPA, —— first-order theory.

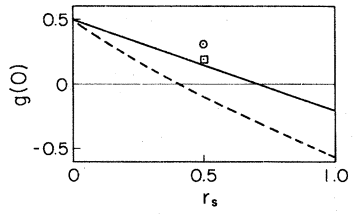

FIG. 12. The value of the pair correlation function at zero interparticle separation vs r_s: – – – – – RPA, —— first-order theory. The points are the results of STLS ⊙, Hubbard ⊡ (Ref. 3).

satisfactorily by all the approximations. There is another relation[4] satisfied by the derivative of $g(r)$:

$$\frac{1}{\sqrt{2}r_s}\frac{dg(r)}{dr}\bigg|_{r\to 0} = g(0)\,, \tag{6.14}$$

which is valid for particles interacting via the Coulomb law.

In an approximate theory (6.14) will be fulfilled only approximately. In the first-order approximation the lhs of (6.14) gives 0.5 which is the value of $g(0)$ at $r_s=0.0$. Thus (6.14) is satisfied with the accuracy to the leading term in r_s of the rhs. The RPA does not satisfy (6.14) at all, since the lhs of (6.14) gives 1.0.

The free-electron correlation function is[9]

$$g_{\rm HF}(r)=1-\frac{J_1^2(r)}{r^2}\,, \tag{6.15}$$

where J_1 is the Bessel function of the first kind of order one. The pair correlation function in different approximations is shown in Fig. 13. The "electrostatic correlation hole" of the RPA is much deeper than that in HFA. This hole is reduced in the first-order approximation. In the first-order theory $g(r)>0$ for $r_s\leq 0.5$ and becomes slightly negative for $r_s=1.0$. $g_{\rm HF}(r)$ and $g_{\rm RPA}(r)$ never exceed 1. In the present approximation $g(r)$ does exceed 1 very slightly, although much less than in the 3D case. The extrema of $g(r)$ are shifted between the different curves ($r_s=0.5$, 1.0) unlike in the 3D case.

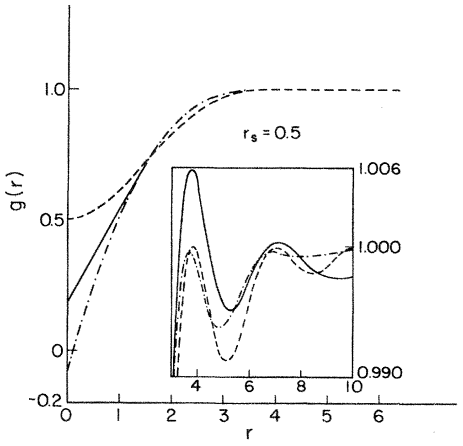

FIG. 13. The pair correlation function $g(r)$ vs r: – – – – – free-electron gas, –·–·–·– RPA for $r_s=0.5$, —— first-order for $r_s=0.5$. r is in units of k_F^{-1}.

VII. CONCLUSIONS

In this paper the contribution of the first-order Feynman diagrams to the proper polarizability, valid for any wave number and frequency, has been evaluated for the first time. A comparison of the results obtained here with the corresponding results in the 3D case shows that there are many qualitative similarities but some important differences too. The latter lie mainly in the nature of singularities of Q^1, e.g., in the 3D case $\mathrm{Im}Q^1$ has jump discontinuities at the "characteristic" frequencies whereas in the 2D case it is singular. $\mathrm{Re}Q^1$ is singular in both cases but in the 2D case the singularity is much stronger. A detailed analysis of the behavior of Q^1 near the singularities has been given.

One of the more interesting results in the 2D electron gas first pointed out by Maldague[13] is a large enhancement of the static polarizability $\pi^1(k)$ at $k\simeq 2k_F$ (see Fig. 8) which could lead to a charge-density wave (CDW) instability in layered transition-metal dichalcogenides. Although higher-order corrections to the polarizability could reduce this enhancement, for values of $r_s\leq 1$, the region of interest in these compounds and where the first-order result should be a reasonable approximation, we tend to believe that this enhancement would persist.

In contrast to the 3D case, the validity of the present perturbation results is confined to the density region $r_s\leq 1$, since already at $r_s=1$ the pair correlation function has become slightly negative for small interparticle separation. This reflects the fact that the effect of correlations for a given r_s is much stronger in a 2D than in a 3D case.

To pursue the perturbation approach beyond what has already been accomplished in this paper seems to be a difficult if not an impossible mathematical task. For the present a more fruitful approach would be a phenomenological one in which one constructs a dynamical complex local field $G(\vec{k},\omega)$ keeping in mind its general behavior as revealed by the first-order perturbation theory and making use of the sum rules. Unfortunately, there is no experimental data available on the dynamical structure factor $S(\vec{k},\omega)$ for a 2D electron liquid to offer some guidance in fixing the parameters of a phenomenological theory. An alternative course is to adopt the equation of motion approach[17] which has had some success in the 3D case.

ACKNOWLEDGMENTS

This work was supported in part under National Science Foundation-Materials Research Laboratories program through the Materials Research Center of Northwestern University (Grant No. DMR 76-80847) and in part by the National Science Foundation Grant No. DMR 77-09937.

APPENDIX A: EVALUATION OF $\mathrm{Im}F^{\mathrm{SE}}$

We first evaluate the imaginary part of the function

$$F^{\mathrm{SE}}(\vec{k},\omega)=-\tfrac{1}{2}\int \frac{d^2p\,d^2p'}{|\vec{p}-\vec{p}'|}\frac{(n^0_{\vec{p}}-n^0_{\vec{p}+\vec{k}})(n^0_{\vec{p}'}-n^0_{\vec{p}'+\vec{k}})}{(\omega+\omega_{\vec{p}}-\omega_{\vec{p}+\vec{k}}+i\eta)^2}\ , \tag{A1}$$

where $n^0_{\vec{p}}=\Theta(1-p^2)$ and

$$\omega_{\vec{p}}=\tfrac{1}{2}\vec{p}^{\,2}\ .$$

Using the identities

$$\frac{1}{(\omega+x)^2}=-\frac{\partial}{\partial\omega}\frac{1}{(\omega+x)}$$

and

$$\frac{1}{(\omega-\omega_0+i\eta)}=P\frac{1}{(\omega-\omega_0)}-i\pi\delta(\omega-\omega_0)\ ,$$

and changing $\vec{p}+\vec{k}\to-\vec{p}$ and $\vec{p}'+\vec{k}\to-\vec{p}'$, (A1) can be written as

$$\mathrm{Im}F^{\mathrm{SE}}(\vec{k},\omega)=\mathrm{Im}[F^{\mathrm{SE}}_A(\vec{k},\omega)+F^{\mathrm{SE}}_B(\vec{k},\omega)]-\mathrm{Im}[F^{\mathrm{SE}}_A(\vec{k},-\omega)+F^{\mathrm{SE}}_B(\vec{k},-\omega)]\ , \tag{A2}$$

where

$$\mathrm{Im}F^{\mathrm{SE}}_A(\vec{k},\omega)=\frac{-\pi}{2}\frac{\partial}{\partial\omega}\int\frac{d^2p\,d^2p'}{|\vec{p}-\vec{p}'|}n^0_{\vec{p}}n^0_{\vec{p}'}\times\delta(\omega+\omega_{\vec{p}}-\omega_{\vec{p}+\vec{k}}) \tag{A3}$$

and

$$\mathrm{Im}F^{\mathrm{SE}}_B(\vec{k},\omega)=\frac{\pi}{2}\frac{\partial}{\partial\omega}\int\frac{d^2p\,d^2p'}{|\vec{p}+\vec{p}'+\vec{k}|}n^0_{\vec{p}}n^0_{\vec{p}'}\times\delta(\omega+\omega_{\vec{p}}-\omega_{\vec{p}+\vec{k}})\ . \tag{A4}$$

Consider the function

$$I(q)=\tfrac{1}{4}\int\frac{d^2p\,n^0_{\vec{p}}}{|\vec{p}-\vec{q}|}\ . \tag{A5}$$

Let $\vec{p}-\vec{q}=\vec{p}$; then

$$I(q)=\tfrac{1}{4}\int_0^\infty\frac{p\,dp}{p}\int_0^{2\pi}d\phi\,\Theta(1-(\vec{p}+\vec{q})^2)=\tfrac{1}{4}\int_0^{2\pi}d\phi\int_0^{p_{\max}}dp\ , \tag{A6}$$

where $p_{\max}$ is determined by $(\vec{p}+\vec{q})^2=1$. For $q<1$, we find

$$I(q)=E(q)\ , \tag{A7}$$

where $E(q)$ is the complete elliptic integral of the second kind. For $q>1$, we find

$$I(q)=\frac{1-q^2}{q}K(1/q)+qE(1/q)\ , \tag{A8}$$

where $K(x)$ is the complete elliptic integral of the first kind.

Now consider the function

$$J(\vec{k},\omega)=\int d^2p\ n^0_{\vec{p}}\delta(\omega+\omega_{\vec{p}}-\omega_{\vec{p}+\vec{k}})\times f\left[\omega,p^2,\frac{\vec{k}\cdot\vec{p}}{k}\right]\ . \tag{A9}$$

Remembering the definition of ν [Eq. (2.8) of the text] we have

$$J(\vec{k},\omega)=\frac{1}{k}\int_0^1 p\,dp\int_0^{2\pi}d\phi\,\delta(\nu-p\cos\phi)\times f(\omega,p^2,p\cos\phi)\ . \tag{A10}$$

Performing the δ integration and introducing a new variable $Z=[(p^2-\nu^2)/(1-\nu^2)]^{1/2}$, we have

$$J(\vec{k},\omega)=\frac{2}{k}\Theta(1-\nu^2)(1-\nu^2)^{1/2}\times\int_0^1 dz\,f(\omega,\nu^2+(1-\nu^2)z^2,\nu)\ . \tag{A11}$$

On using (A5) in (A3) and (A4) and then using (A9) and (A11) we find

$$\mathrm{Im}[F_A^{\mathrm{SE}}(\vec{k},\omega)+F_B^{\mathrm{SE}}(\vec{k},\omega)]=\frac{4\pi}{k^2}\frac{\partial}{\partial\nu}\left[\Theta(1-\nu^2)(1-\nu^2)^{1/2}\int_0^1 dz\,[I(p_1)-I(p_2)]\right], \tag{A12}$$

where

$$p_1=[(\nu+k)^2+(1-\nu^2)z^2]^{1/2}=p(k,\nu,z)$$

and

$$p_2=p(0,\nu,z)\ .$$

Performing the ν differentiation in (A12) and using the relation

$$\frac{d}{dz}I(P(k,\nu,z))=I'(p)\frac{(1-\nu^2)z}{p}\ , \tag{A13}$$

and integrating the result by parts, then using (2.8) and (A2) we find

$$\mathrm{Im}F^{\mathrm{SE}}(\vec{k},\omega)=\Theta(1-\nu_+^2)\phi^{\mathrm{SE}}(k,\nu_+)-\Theta(1-\nu_-^2)\phi^{\mathrm{SE}}(k,\nu_-)\ , \tag{A14}$$

where

$$\phi^{\mathrm{SE}}(k,\nu)=\frac{4\pi}{k^2}\left[\frac{-\nu}{(1-\nu^2)^{1/2}}\{I([(k+\nu)^2+(1-\nu^2)]^{1/2})-1\}\right.$$
$$\left.+(1-\nu^2)^{1/2}\left[(k+\nu)\int_0^1 dz\frac{I'(p_1)}{p_1}-\nu\int_0^1 dz\frac{I'(p_2)}{p_2}\right]\right]. \tag{A15}$$

APPENDIX B: EVALUATION OF $\mathrm{Im}F^{\mathrm{ex}}$

Here we wish to evaluate the imaginary part of the function

$$F^{\mathrm{ex}}(\vec{k},\omega)=\tfrac{1}{2}\int\frac{d^2p\,d^2p'}{|\vec{p}-\vec{p}'|}\frac{(n^0_{\vec{p}}-n^0_{\vec{p}+\vec{k}})(n^0_{\vec{p}'}-n^0_{\vec{p}'+\vec{k}})}{(\omega+\omega_{\vec{p}}-\omega_{\vec{p}+\vec{k}}+i\eta)(\omega+\omega_{\vec{p}'}-\omega_{\vec{p}'+\vec{k}}+i\eta)}\ . \tag{B1}$$

Following the procedure adopted in the calculation of F^{SE}, (B1) becomes

$$\mathrm{Im}F^{\mathrm{ex}}(\vec{k},\omega)=\mathrm{Im}[F_A^{\mathrm{ex}}(\vec{k},\omega)+F_B^{\mathrm{ex}}(\vec{k},\omega)]-\mathrm{Im}[F_A^{\mathrm{ex}}(\vec{k},-\omega)+F_B^{\mathrm{ex}}(\vec{k},-\omega)]\ , \tag{B2}$$

where

$$\mathrm{Im}F_A^{\mathrm{ex}}(\vec{k},\omega)=-\pi\int d^2p\,n^0_{\vec{p}}\,\delta(\omega+\omega_{\vec{p}}-\omega_{\vec{p}+\vec{k}})\mathscr{P}\int\frac{d^2p'n^0_{\vec{p}'}}{|\vec{p}-\vec{p}'|}\frac{1}{\omega+\omega_{\vec{p}'}-\omega_{\vec{p}'+\vec{k}}} \tag{B3}$$

and

$$\mathrm{Im}F_B^{\mathrm{ex}}(\vec{k},\omega)=\pi\int d^2p\,n^0_{\vec{p}}\,\delta(\omega+\omega_{\vec{p}}-\omega_{\vec{p}+\vec{k}})\mathscr{P}\int\frac{d^2p'n^0_{\vec{p}'}}{|\vec{p}+\vec{p}'+\vec{k}|}\frac{1}{\omega+\omega_{\vec{p}'+\vec{k}}-\omega_{\vec{p}'}}\ . \tag{B4}$$

Let us consider the function

$$G(\zeta,q^2,\hat{n}\cdot\vec{q})=\mathscr{P}\int\frac{d^2p\,n^0_{\vec{p}}}{|\vec{p}-\vec{q}|}\frac{1}{\zeta-\hat{n}\cdot\vec{p}}\ . \tag{B5}$$

We take a coordinate system such that $\hat{n}=(1,0)$, $\vec{q}=(q_1,q_2)$, and $\vec{p}=(x,y)$. Performing the y integration, we obtain

$$G(\zeta,q^2,q_1)=\mathscr{P}\int_{-1}^{+1}\frac{dx}{(\zeta-x)}[R((x-q_1)^2,(1-x^2)^{1/2}-q_2)-R((x-q_1)^2,-(1-x^2)^{1/2}-q_2)]\ . \tag{B6}$$

where

$$R(a,\rho)=\ln[\rho+(a^2+\rho^2)^{1/2}]\ . \tag{B7}$$

Let us again introduce another function

$$S(w,b,c,)=\int_0^1 dz\, R(w,b-cz)=\frac{1}{c}[H(w,b)-H(w,b-c)]\ , \tag{B8}$$

where

$$H(w,y)=y\ln[y+(w^2+y^2)^{1/2}]-(w^2+y^2)^{1/2}\ . \tag{B9}$$

Using (B5) in (B3) and (B4), we obtain an expression which has the structure of (A9). Following the procedure adopted in Appendix A and after some lengthy algebra we obtain

$$\mathrm{Im}F^{\mathrm{ex}}(\vec{k},\omega)=\Theta(1-\nu_+^2)\phi^{\mathrm{ex}}(k,\nu_+)-\Theta(1-\nu_-^2)\phi^{\mathrm{ex}}(k,\nu_-)\ , \tag{B10}$$

where

$$\phi^{\mathrm{ex}}(k,\nu)=\frac{2\pi}{k^2}\left[\mathscr{P}\int_{-1}^{+1}\frac{dx}{\nu+k-x}T((k+\nu-x),(1-x^2)^{1/2},(1-\nu^2)^{1/2})\right.$$
$$\left.-\mathscr{P}\int_{-1}^{+1}\frac{dx}{\nu-x}T((\nu-x),(1-x^2)^{1/2},(1-\nu^2)^{1/2})\right] \tag{B11}$$

where

$$T(W,X,N)=[W^2+(X-N)^2]^{1/2}-[W^2+(X+N)^2]^{1/2}-(X-N)\ln\left|\frac{[W^2+(X-N)^2]^{1/2}+X-N}{W}\right|$$
$$-(X+N)\ln\left|\frac{[W^2+(X+N)^2]^{1/2}-X-N}{W}\right|\ . \tag{B12}$$

(For algebraic details see Ref. 12.)

APPENDIX C: EVALUATION OF $G_{\mathrm{HF}}^{\infty}(k)$

G_{HF}^{∞} is given by Eq. (5.16) of the text and is

$$G_{\mathrm{HF}}^{\infty}(\vec{k})=\frac{1}{2\pi k^3}\int d^2q\frac{(\vec{k}\cdot\vec{q})^2}{q}[S_{\mathrm{HF}}(q)-S_{\mathrm{HF}}(|\vec{k}+\vec{q}|)] \tag{C1}$$

$$=\frac{1}{2\pi k^3}\int d^2q\frac{(\vec{k}\cdot\vec{q})^2}{q}[S_{\mathrm{HF}}(q)-1]+\frac{1}{2\pi k^3}\int d^2q\frac{(\vec{k}\cdot\vec{q})^2}{q}[1-S_{\mathrm{HF}}(|\vec{k}+\vec{q}|)]\ . \tag{C2}$$

Changing $\vec{k}+\vec{q}\rightarrow-\vec{q}$ in the second term of (C2) we get

$$G_{\mathrm{HF}}^{\infty}(\vec{k})=\frac{1}{2\pi k}\int_0^{\infty}q\,dq[1-S_{\mathrm{HF}}(q)][Z(q,k)-Z(q,0)]\ , \tag{C3}$$

where

$$Z(q,k)=2\int_0^{\pi}d\phi\frac{(q\cos\phi+k)^2}{(q^2+k^2+2qk\cos\phi)^{1/2}}\ . \tag{C4}$$

If we now introduce the new variable $x=\sin(\phi/2)$, (C4) can be expressed in terms of complete elliptic integrals:

$$Z(q,k)=\frac{2}{3}\frac{k+q}{k^2}[K(\tilde{q})(q-k)^2$$
$$+E(\tilde{q})(5k^2-q^2)]\ , \tag{C5}$$

where

$$\tilde{q}=\left[\frac{4qk}{(q+k)^2}\right]^{1/2}$$

and $Z(q,0)=\pi q$. Thus

$$G_{\mathrm{HF}}^{\infty}(\vec{k})=\frac{1}{2\pi k}\int_0^{\infty}q\,dp[1-S_{\mathrm{HF}}(q)]$$
$$\times[Z(q,k)-\pi q]\ . \tag{C6}$$

The q integration in (C6) has to be done numerically.

APPENDIX D: EVALUATION OF THE CONSTANT C IN THE SMALL-WAVELENGTH EXPANSION OF $S(k)$

In the limit $k\to\infty$, the relation $|Q^0+Q^1|<<1$ is fulfilled in general except in the narrow frequency regions close to $\omega_s^{\pm}(k)$. Thus the integrand in Eq. (6.9) of the text can be expanded in almost the whole range of integration as

$$-\frac{1}{1+Q}=-1+Q^0+Q^1-(Q^0)^2+\cdots . \tag{D1}$$

Thus

$$\int_0^\infty d\omega\,\mathrm{Im}\left[\frac{-1}{1+Q}\right]=\int_0^\infty d\omega\,\mathrm{Im}Q^0 - \int_0^\infty d\omega\,\mathrm{Im}[(Q^0)^2] + \int_0^\infty d\omega\,\mathrm{Im}[Q^1]+O\left[\frac{1}{k^5}\right] . \tag{D2}$$

Now

$$\int_0^\infty d\omega\,\mathrm{Im}Q^0=\frac{\pi r_s}{\sqrt{2}k} \quad \text{for } k>2 \tag{D3}$$

and

$$\int_0^\infty d\omega\,\mathrm{Im}[(Q^0)^2]=\frac{\pi r_s^2}{k^4}\left[1+O\left[\frac{1}{k^2}\right]\right] . \tag{D4}$$

Denote

$$\lim_{k\to\infty}\int_0^\infty d\omega\,\mathrm{Im}Q^1(\vec{k},\omega)=I_{\vec{k}} . \tag{D5}$$

To calculate (D5), the methods of Appendixes A and B are used. Since

$$Q^1(\vec{k},\omega)=\frac{\alpha_D^2}{k}[F^{\mathrm{SE}}(\vec{k},\omega)+F^{\mathrm{ex}}(\vec{k},\omega)] ,$$

$$I_{\vec{k}}=I_{\vec{k}}^{\mathrm{SE}}+I_{\vec{k}}^{\mathrm{ex}} ,$$

where

$$I_{\vec{k}}^{\mathrm{SE}}=-\frac{\pi}{2}\frac{r_s^2}{2\pi^2 k}\int\frac{d^2p\,d^2p'}{|\vec{p}-\vec{p}'|}(n^0_{\vec{p}}-n^0_{\vec{p}+\vec{k}})(n^0_{\vec{p}'}-n^0_{\vec{p}'+\vec{k}})\int_0^\infty\frac{\partial}{\partial\omega}\delta(\omega+\omega_{\vec{p}}-\omega_{\vec{p}+\vec{k}})d\omega=0 . \tag{D6}$$

$$I_{\vec{k}}^{\mathrm{ex}}=\frac{-\pi r_s^2}{2\pi^2 k}\int\frac{d^2p\,d^2p'}{|\vec{p}-\vec{p}'|}(n^0_{\vec{p}}-n^0_{\vec{p}+\vec{k}})(n^0_{\vec{p}'}-n^0_{\vec{p}'+\vec{k}})\mathscr{P}\int_0^\infty\frac{d\omega\,\delta(\omega+\omega_{\vec{p}'}-\omega_{\vec{p}'+\vec{k}})}{\omega+\omega_{\vec{p}}-\omega_{\vec{p}+\vec{k}}}$$
$$=\frac{-r_s^2}{2\pi k}\int\frac{d^2p\,d^2p'}{|\vec{p}-\vec{p}'|}\frac{(n^0_{\vec{p}}-n^0_{\vec{p}+\vec{k}})(n^0_{\vec{p}'}-n^0_{\vec{p}'+\vec{k}})\Theta(\vec{p}'\cdot\vec{k}+k^2/2)}{\vec{p}'\cdot\vec{k}-\vec{p}\cdot\vec{k}} . \tag{D7}$$

The Θ function takes care of the fact that the zero of the δ function is in the region of the ω integration. Following the procedure of Appendix A, (D7) can be written as the sum of four terms. Three of these terms become zero, and the surviving term is

$$(I)_{\vec{k}}^{\mathrm{ex}}=\frac{r_s^2}{2\pi k}\int\frac{d^2p\,d^2p'n^0_{\vec{p}}n^0_{\vec{p}'}\Theta(\vec{p}'\cdot\vec{k}+k^2/2)}{|\vec{p}+\vec{p}'+\vec{k}|(\vec{p}+\vec{p}'+\vec{k})\cdot\vec{k}} . \tag{D8}$$

In the limit $k\to\infty$, (D8) becomes

$$I_k^{\mathrm{ex}}=\frac{r_s^2}{2\pi k}\frac{1}{k^3}\int_{|\vec{p}|<1}d^2p\int_{|\vec{p}'|<1}d^2p'=\frac{\pi}{2}\frac{r_s^2}{k^4} , \tag{D9}$$

Therefore

$$\lim_{k\to\infty}\int_0^\infty d\omega\,\mathrm{Im}Q^1(\vec{k},\omega)=\frac{\pi}{2}\frac{r_s^2}{k^4} . \tag{D10}$$

Now

$$C=\lim_{k\to\infty}\left\{k^3\left[\frac{\sqrt{2}}{\pi}\frac{k}{r_s}\int_0^\infty d\omega\,\mathrm{Im}\left[-\frac{1}{1+Q}\right]-1\right]\right\} . \tag{D11}$$

[See Eq. (6.9) of the text.] Using (D3), (D4), (D10), and (D2) in (D11) we obtain

$$C=\left\{k^3\left[\frac{\sqrt{2}}{\pi}\frac{k}{r_s}\left[\frac{\pi r_s}{\sqrt{2}k}-\frac{\pi r_s^2}{k^4}+\frac{\pi}{2}\frac{r_s^2}{k^4}\right]-1\right]\right\} .$$

Thus

$$C=\sqrt{2}r_s(-1+\tfrac{1}{2}) . \tag{D12}$$

*Permanent address: Institute of Nuclear Research, Swierk, 05-400 Otwock, Poland.

[1]F. Stern, Phys. Rev. Lett. 18, 546 (1967).
[2]A. K. Rajagopal, Phys. Rev. B 15, 4264 (1977).
[3]M. Jonson, J. Phys. C 9, 3055 (1976).
[4]A. K. Rajagopal and J. C. Kimball, Phys. Rev. B 15, 2819 (1977).
[5]K. S. Singwi, M. P. Tosi, R. H. Land, and A. Sjölander, Phys. Rev. 176, 589 (1968).
[6]A. Holas, P. K. Aravind, and K. S. Singwi, Phys. Rev. B 20, 4912 (1979).
[7]R. K. P. Zia, J. Phys. C 6, 3121 (1973).
[8]M. Apostol and P. Solomon, Rev. Roum. Phys. 20, 15 (1975).
[9]M. L. Glasser, J. Phys. C 10, L121 (1977).
[10]K. N. Pathak and P. Vashishta, Phys. Rev. B 7, 3649 (1973).
[11]D. J. W. Geldart and R. Taylor, Can. J. Phys. 48, 155 (1970).
[12]S. R. Sharma, Ph.D. thesis, Northwestern University, 1982 (unpublished).
[13]P. F. Maldague, Solid State Commun., 26, 133 (1978).
[14]D. Pines, *Elementary Excitations in Solids* (Benjamin, New York, 1964).
[15]D. Pines and P. Nozières, *The Theory of Quantum Liquids* (Benjamin, New York, 1963).
[16]J. C. Kimball, Phys. Rev. A 7, 1648 (1973).
[17]P. K. Aravind, A. Holas, and K. S. Singwi, Phys. Rev. B 25, 561 (1982).